

Control of nanomaterial self-assembly in ultrasonically levitated droplets

Article

Published Version

Open access article published under an ACS AuthorChoice License, which permits copying and redistribution of the article or any adaptations for non-commercial purposes.

Seddon, A. M., Richardson, S. J., Rastogi, K., Plivelic, T. S., Squires, A. M. and Pfrang, C. (2016) Control of nanomaterial self-assembly in ultrasonically levitated droplets. *Journal of Physical Chemistry Letters*, 7 (7). pp. 1341-1345. ISSN 1948-7185 doi: 10.1021/acs.jpcllett.6b00449 Available at <https://centaur.reading.ac.uk/62115/>

It is advisable to refer to the publisher's version if you intend to cite from the work. See [Guidance on citing](#).

To link to this article DOI: <http://dx.doi.org/10.1021/acs.jpcllett.6b00449>

Publisher: American Chemical Society

All outputs in CentAUR are protected by Intellectual Property Rights law, including copyright law. Copyright and IPR is retained by the creators or other copyright holders. Terms and conditions for use of this material are defined in the [End User Agreement](#).

www.reading.ac.uk/centaur

CentAUR

Central Archive at the University of Reading

Reading's research outputs online

Control of Nanomaterial Self-Assembly in Ultrasonically Levitated Droplets

Annala M. Seddon,^{†,§} Sam J. Richardson,[‡] Kunal Rastogi,[‡] Tomás S. Plivelic,[⊥] Adam M. Squires,^{*,‡} and Christian Pfrang^{*,‡}

[†]H.H. Wills Physics Laboratory, University of Bristol, Tyndall Avenue, Bristol BS8 1TL, United Kingdom

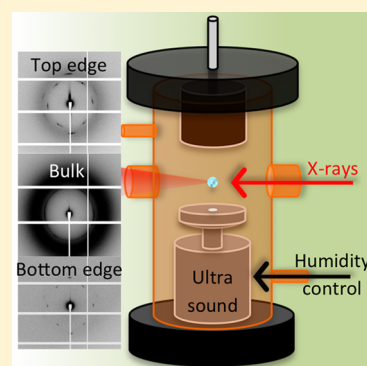
[§]Bristol Centre for Functional Nanomaterials, H.H. Wills Physics Laboratory, University of Bristol, Tyndall Avenue, Bristol BS8 1TL, United Kingdom

[‡]Department of Chemistry, University of Reading, Whiteknights Campus, Reading RG6 6AD, United Kingdom

[⊥]MAX IV Laboratory, Lund University, 22100 Lund, Sweden

S Supporting Information

ABSTRACT: We demonstrate that acoustic trapping can be used to levitate and manipulate droplets of soft matter, in particular, lyotropic mesophases formed from self-assembly of different surfactants and lipids, which can be analyzed in a contact-less manner by X-ray scattering in a controlled gas-phase environment. On the macroscopic length scale, the dimensions and the orientation of the particle are shaped by the ultrasonic field, while on the microscopic length scale the nanostructure can be controlled by varying the humidity of the atmosphere around the droplet. We demonstrate levitation and in situ phase transitions of micellar, hexagonal, bicontinuous cubic, and lamellar phases. The technique opens up a wide range of new experimental approaches of fundamental importance for environmental, biological, and chemical research.



Levitation is an elegant method allowing contact-less manipulation and analysis of individual particles. Acoustic (ultrasonic) levitation^{1,2} has been shown to be a powerful and versatile technique. It was first developed for microgravity applications in space³ but has found a range of applications studying liquid^{4–6} and solid^{7,8} particles in a wall-less environment investigating phenomena such as liquid mixing and ice crystallization.

The principle behind ultrasonic trapping is that a standing acoustic wave is created between a transmitter (oscillating at a given frequency) and a reflector; within this standing wave there are several pressure nodes that allow stable levitation of the sample of interest. Alteration of the distance between transducer and reflector allows the number of and distance between the pressure nodes to be varied. Attractive features of acoustic levitation include a compact, portable design, the requirement for very small sample volumes (typically 5–10 μL), and the ability to introduce contact-less mixing⁹ and to change droplet aspect ratio by changing ultrasonic pressure. These features enhance suitability of the levitated sample as a wall-less reactor and enable noncontact measurements of droplet forces, such as surface tension,^{10,11} while the entire droplet surface is subject to a uniform air–liquid interface. Evaporation from aqueous droplets changes the composition and structure of the levitated sample. This has been used to study, for example, protein agglomeration, while the sample was allowed to dry in an open acoustic levitator.¹²

We introduce a controlled gas-phase environment and show that the relative humidity (RH) can be used to control condensation and evaporation to and from the droplet. In this way we can access a desired phase in soft matter and furthermore induce phase transitions. Manipulation of soft matter nanostructure by changing composition through humidity control has not hitherto been carried out in a contactless manner. Recently, humidity control of lyotropic liquid crystalline phases has been applied to soft crystals¹³ and thin films,^{14,15} in both cases supported on solid substrates potentially introducing surface effects. The application of ultrasonic levitation to soft matter droplets has, to our knowledge, not been previously reported.

A further advantage of the contact-less sample environment offered by ultrasonic levitation is the ready application of different analytical techniques. It has been combined with methods such as FTIR, Raman spectroscopy, and microscopy as well as UV–visible spectroscopy.^{16–20} There are few examples of the coupling of ultrasonic levitation with small-angle X-ray scattering (SAXS); it has been applied to the study of the growth mechanism of inorganic and organic crystals,^{21,22} the agglomeration of soluble proteins,¹² and the structures of glassy materials.²³ It is reasonably straightforward to combine

Received: February 25, 2016

Accepted: March 15, 2016

several techniques with ultrasonic levitation to analyze the same sample simultaneously. Here we combine synchrotron SAXS with in situ optical imaging of the levitated droplet.

We describe the use of ultrasonic levitation to investigate lyotropic liquid crystals. These viscous self-assembled materials comprise a range of 2D and 3D nanostructures, and they are important from a wide variety of biological, commercial, and nanotechnological perspectives. “Type I” liquid crystals are typically formed by self-assembly of commercial surfactants and detergents into spherical or cylindrical micelles surrounded by water (“normal topology” phases) or into stacks of bilayers (“lamellar” phases).²⁴ Biological lipid molecules can also form lamellar phases; the constituent lipid bilayers form the structural basis of cell membranes. In addition, lipid molecules adopt structures representing a variety of nonlamellar inverted analogues of their type I counterparts (“inverse topology” or “type II” phases).²⁵ These contain spheres, cylinders, or 3D networks of water surrounded by lipid in the inverse micellar (L_{II}), inverse hexagonal (H_{II}), and inverse bicontinuous cubic (Q_{II}) phases, respectively. Self-assembly of biological liquid crystalline phases is of importance from the perspective both of fundamental knowledge of the cell membrane and in applications for biological research; the Q_{II} phase has been shown to be an excellent host matrix for the growth of membrane protein crystals²⁶ and is the subject of investigation as a medium for drug delivery.²⁷ Finally, mesoporous metals have been produced by deposition within a range of normal and inverse topology templates including hexagonal²⁸ and inverse cubic phases.²⁹

Transformations between these liquid-crystalline phases are typically monitored using small-angle X-ray scattering (SAXS), often induced by changing temperature,³⁰ although studies have been carried out on phase transitions induced by changes in hydration,³¹ pressure,³² additives,³³ and humidity.¹⁴ Experiments are usually carried out on bulk polydomain samples in sealed cells, although humidity response has been measured with thin-film samples, supported on a substrate, exposed to a humidified gaseous environment, and analyzed with grazing-incidence SAXS. This has been carried out on highly oriented lamellar phases (stacks of lipid bilayers), whose spacing depends on humidity,³⁴ and more recently we have used controlled humidity to study diamond (Q_{II}^D) and gyroid (Q_{II}^G) inverse bicontinuous cubic phases in thin films that also show high degrees of alignment.^{14,15} In such cases there are likely to be strong interfacial effects,¹⁴ and it is very difficult to separate the influences of the two interfaces: with the solid substrate and with the humidified environment. Even in more conventional experiments in sealed cells it is impossible to avoid wall effects. These effects can be avoided when levitating the sample.

Here we describe a new type of experimental setup (see Figure 1), where ultrasonic levitation is carried out within a controlled gas-phase environment and combined with SAXS analysis. We studied droplets of lyotropic liquid crystals in this contactless sample environment, where the relative humidity of the surrounding atmosphere was used to control the phase, and to induce phase changes that could be analyzed in real time. Taking advantage of the fact that there were no walls in contact with the sample, we were able to demonstrate interfacial effects at the surfaces of the droplet, which in some cases exhibit high degrees of orientation of the surfactant mesophase and a difference in composition and phase compared with the droplet core. We have selected several different amphiphile systems to show that a representative range of type I and type II lyotropic

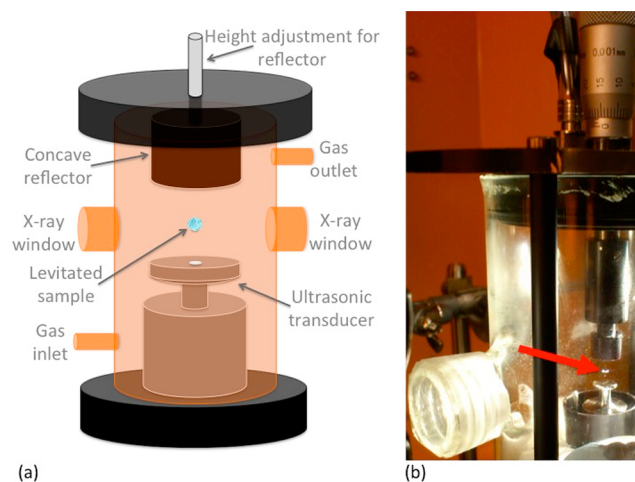


Figure 1. Experimental setup: (a) schematic diagram of ultrasonic levitator contained in a flow-through environmental chamber and (b) photograph of the setup at MAX-lab with a levitated droplet (see red arrow).

phases can be levitated and analyzed. The molecules (see [Experimental Methods](#) for details) include the lipids phytantriol and Rylo that formed the inverse micellar, Q_{II}^G and Q_{II}^D phases on increasing humidity,³⁵ the nonionic detergent Brij-56 that showed the lamellar and micellar phases, and a mixture of surfactants oleic acid and sodium oleate (1:1 weight ratio in a 3% w/w solution of 1 wt % NaCl solution) that formed the normal topology hexagonal phase.

The different surfactants in pure form and as lyotropic phases have very different physical properties requiring varying strategies to produce small droplets in the levitator. For the lipids phytantriol and Rylo, the lipid/water Q_{II} phases are highly viscous, as is pure phytantriol, while Rylo is a hygroscopic solid, so neither form of either lipid could be injected directly into the levitator. Furthermore, in an open environment, the lipids only form Q_{II}^G and Q_{II}^D phases at very high relative humidities, so glycerol was added as a humectant.³⁵ Mixtures of phytantriol/glycerol (80:20 w/w) and Rylo/glycerol (68:32 w/w)³⁵ prepared as ethanolic solutions (each containing 50% ethanol by weight) were injected into the levitator as $\sim 5 \mu\text{L}$ droplets; the ethanol evaporated to leave a droplet of lipid/glycerol mixture that took up water from the humidified environment to adopt the different Q_{II} phases. The sodium oleate/oleic acid/brine system was a liquid of sufficiently low viscosity that it could be injected directly into the levitator. Brij-56 is a waxy solid at room temperature, small grains of which could be placed directly into the levitator, and because it is very hygroscopic it then also took on water from the surrounding humidified environment to undergo phase transitions. Alternatively, a suspension of 20% w/w Brij-56 in water forms a micellar phase,³⁶ which is also sufficiently liquid to be injected directly. This then dehydrated to form hexagonal and lamellar lyotropic phases.

Levitated droplets were in most cases found to be of ellipsoidal shape with typical droplet dimensions 0.5 to 1 mm vertically and 1.8 to 2 mm horizontally. The aspect ratio could be altered by adjusting the transducer–reflector distance or the sound pressure. In addition, we could levitate smaller particles, several hundred microns in diameter, which tended to be more spherical. Furthermore, vertical strings of droplets trapped in different nodes could be levitated. Some representative

examples are shown in Figure S1 in the Supporting Information.

Figure 2 (right-hand column) shows representative 2D images obtained from SAXS experiments on acoustically

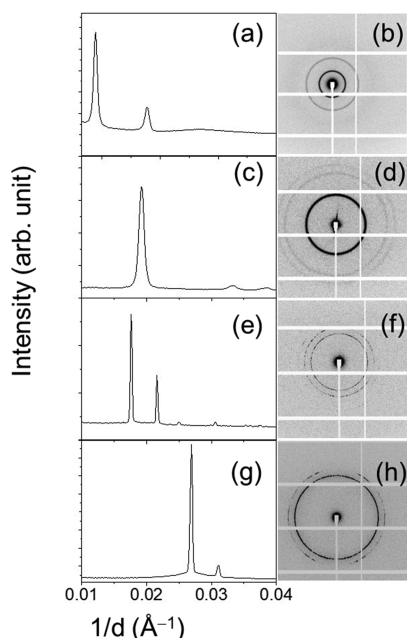


Figure 2. Integrated and 2D SAXS data taken from levitated droplets showing a range of lyotropic phases measured: (a,b) lamellar phase from Brij-56 (RH = 67%); (c,d) hexagonal phase from 1:1 oleic acid/sodium oleate initially 3 wt % in 1 wt % NaCl solution (RH = 84%); (e,f) Q_{II}^D phase from Rylo/glycerol (RH > 98%); and (g,h) Q_{II}^G phase from phytantriol/glycerol (RH = 83%).

levitated lyotropic liquid crystals. The corresponding 1D integrated plots are shown in the left-hand column. This demonstrates the range of easily accessible phases that can be stably levitated.

Lattice parameters for levitated droplets of the Q_{II}^D phases formed by phytantriol and Rylo with glycerol in high humidity are comparable to those measured previously on thin films using GI-SAXS (see Table 1), which themselves agreed with

Table 1. Lattice Parameters Obtained through SAXS from Ultrasonically Levitated Droplets Compared with Literature Values from Thin Films

sample	phase	lattice parameter (Å)
phytantriol/glycerol (80:20 w/w), >95% RH	Q_{II}^D	67.5 ± 0.2 (this work)
		67 ± 1 (Richardson et al., 2015) ³⁵
Rylo/glycerol (68:32 w/w), >95% RH	Q_{II}^D	80.0 ± 0.3 (this work)
		81–86 (Rittman et al., 2013) ¹⁵
		87 ± 1 (Richardson et al., 2015) ³⁵

literature values for lipid/water mixtures under excess water conditions, in the absence of glycerol.³⁵ (Discrepancies in the case of Rylo probably reflect sample-to-sample variation due to different levels of contamination in this industrial-grade material.¹⁵) This indicates that acoustically levitating droplets of sample do not significantly affect the nanostructure adopted by the lyotropic phase.

By controlling the relative humidity in the chamber, we can effectively change the water content of the levitated droplet in

equilibrium with the surrounding water vapor and therefore control the lyotropic phase adopted, and we can induce phase transitions that can be monitored in real time using time-resolved SAXS. An example of this is shown in Figure 3, where

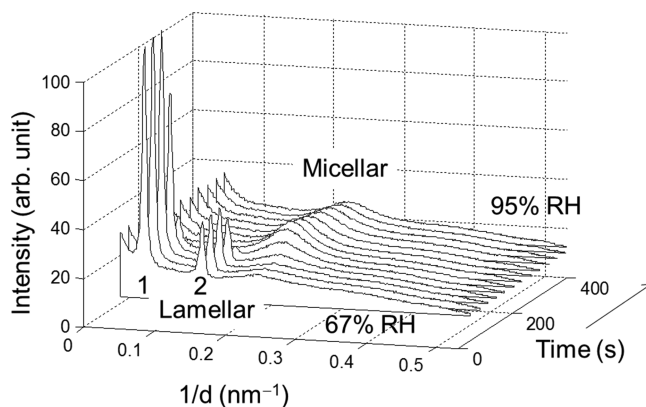


Figure 3. Time-resolved 1D SAXS data showing a phase transition from lamellar to micellar in the Brij-56 system under increasing humidity. The first- and second-order reflections of the lamellar phase are labeled.

a transformation from a lamellar to a micellar phase of the type I surfactant Brij-56 ($C_{16}EO_{10}$) is induced by changing the surrounding relative humidity from 67 to 95%. Similar transformations between L_{II} and Q_{II}^D phases in type II systems are shown in the Supporting Information (Figure S2).

We exploited the fact that the X-ray beam dimensions (0.3×0.3 mm) were smaller than those of the droplet (up to 2×1 mm), allowing scans horizontally and vertically through the levitated sample. Variations in droplet composition could be seen, in particular, when using larger droplets or relatively rapid changes in RH. On increasing RH for type II lipids, it was common to observe the development of a core-shell structure comprising a micellar phase on which a shell of Q_{II}^D phase would gradually form, as illustrated in Figure 4. The sharp Q_{II}^D reflections are present throughout because the X-ray beam always interacts with the shell of the droplet, whether it is passing through the front and back of the sample (when aligned with the center) or glancing through one edge; however, the broad inverse micellar peak becomes more intense as the beam trajectory approaches the center of the droplet (Figure 4).

Interestingly, when the X-ray beam passes through the top or bottom edge of a levitated droplet with such a Q_{II}^D shell, a high degree of alignment can often be seen in 2D SAXS images, as shown in Figure 4. These highly oriented patterns in every case demonstrated an approximately vertical [111] direction, that is, normal to the cubic phase/vapor interface, as shown by the more intense on-axis (vertical) reflection in the second ring. (See Figure 4a,c.)

Calculations³⁷ have shown (111) to be the most thermodynamically stable facet for a Q_{II}^D phase. This has also been observed from grazing-incidence SAXS data from thin films.¹⁴ In that experiment,¹⁴ it was not possible to separate effects from the two different interfaces, with the vapor phase and the substrate lying above and below the Q_{II}^D phase films. In levitated droplets, because there are no other interfaces, we can rule out substrate interface effects.

However, we must take into account additional effects due to the ultrasonic field itself, which may also orient a particular axis in the vertical direction. To study these two competing effects,

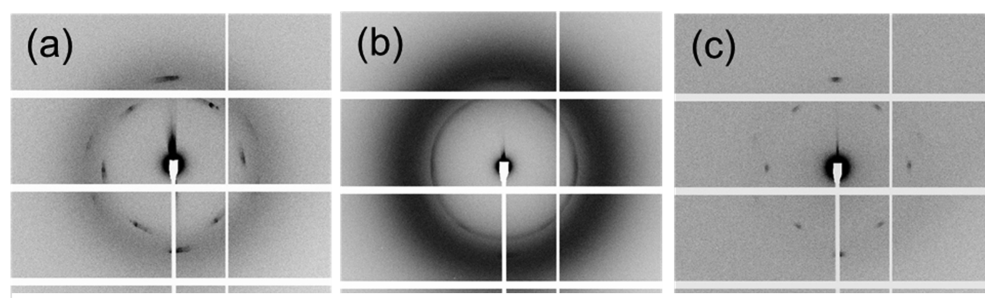


Figure 4. 2D SAXS patterns from the edges and center of an acoustically levitated droplet formed from phytantriol in 20% glycerol at a relative humidity of 75%: (a) top, (b) center, and (c) bottom.

we carried out horizontal scans to investigate the sides of the droplets. If the orientation shown in Figure 4 was solely due to interfacial effects, we would expect the sides of the droplet to show a pattern that was rotated by 90° compared with that obtained at the top or bottom; conversely, if the orientation was solely due to the (vertical) acoustic field, the pattern would remain unchanged. In fact, neither was observed, and instead the sides showed reduced alignment (Figure S3). This suggests that both the acoustic field and the interfacial effects contribute to the alignment at the top and bottom, whereas these effects act in opposition at the sides.

In summary, we have demonstrated for the first time that (i) droplets of soft nanomaterials can be acoustically levitated and analyzed in a contact-less manner and (ii) we have successfully developed an experimental setup allowing simultaneous SAXS/acoustic levitation in a controlled gas-phase environment. Our study shows that ultrasonic levitation can be applied to a range of different lyotropic liquid crystalline phases formed by different lipids and surfactant molecules, and that the nanostructure can be controlled by changing the humidity of the surrounding atmosphere. We observed a number of new phenomena for lyotropic phases, including shape deformation caused by the ultrasonic field, high degrees of interfacial orientation, and a core-shell morphology reflecting variations in sample hydration. The technique opens up new avenues in experimental approaches of fundamental importance for environmental, biological, and chemical research.

EXPERIMENTAL METHODS

All compounds were used as received. Phytantriol (3,7,11,15-tetramethyl-1,2,3-hexadecanetriol) was obtained from Adina Cosmetic Ingredients (U.K.). Rylo MG-19 (Danisco, Copenhagen, Denmark, approximate purity 90%) is an industrial form of monoolein (2,3-dihydroxypropyl (*Z*)-octadec-9-enoate), which we refer to simply as Rylo in this paper. Glycerol (propane-1,2,3-triol), Brij-56 ($C_{16}H_{33}(OCH_2CH_2)_{10}OH$, also known as polyoxyethylene (10) cetyl ether, C16EO10, or Brij C10), oleic acid, and sodium oleate were purchased from Sigma-Aldrich (U.K.). Our experimental setup is based on a modified commercial levitator (tec5, Oberursel, Germany) with a fixed transducer frequency of 100 kHz and a variable HF power of 0.65 to 5 W. A concave reflector was mounted on a micrometer screw for adjustment of the reflector-transducer distance. The distance between the transducer front face and the reflector was set to ~ 26 mm with a maximum distance variation of ± 6 mm. The levitator was enclosed in a custom-built flow-through Pyrex environmental chamber fitted with X-ray transparent windows and access ports for relative humidity and temperature measurements as well as gas supply and

removal. (See Figure 1.) This chamber was placed in the sample position of beamline I911-4 at MAX-lab. The desired relative humidity was achieved by controlling the ratios of flows of dry and H_2O -saturated O_2 from a gas cylinder. The liquid samples were introduced by means of a microliter syringe (Hamilton). The droplets were detached from the tip of the needle of the syringe by altering the reflector-transducer distance and simultaneously adjusting the sound pressure to stabilize levitated droplets. The levitator was mounted on an x -, y -, z -stage for precise alignment of X-ray beam and levitation zone. SAXS experiments were carried out using a beam size of 0.3×0.3 mm full width at half-maximum. The wavelength was 0.91 \AA and data were collected over a q range of 0.006 to 0.18 \AA^{-1} . Exposure times were typically 30 to 60 s for a typical trapped droplet size of 0.5 to 1 mm vertically and 1.8 to 2 mm horizontally. Data were analyzed using an in-house developed macro.³⁸

ASSOCIATED CONTENT

Supporting Information

The Supporting Information is available free of charge on the ACS Publications website at DOI: [10.1021/acs.jpcllett.6b00449](https://doi.org/10.1021/acs.jpcllett.6b00449).

Photographs showing typical examples of levitated droplets; additional SAXS data showing phase transitions; and 2D SAXS images from the sides of a droplet. (PDF)

AUTHOR INFORMATION

Corresponding Authors

*E-mail: a.m.squires@reading.ac.uk. Tel: +44(0) 118 378 4736.

*E-mail: c.pfrang@reading.ac.uk. Tel: +44(0) 118 378 8789.

Notes

The authors declare no competing financial interest.

ACKNOWLEDGMENTS

Beam time was awarded under MAX-lab Proposal IDs 20120333 and 20140459. Additional funding was awarded under Bio-Struct X travel funding grants 4206 and 9487. C.P. is grateful for expert advice on acoustic levitation from Dr. Ernst G. Lierke. C.P. received financial support for the development of the acoustic levitator from the Royal Society (2007/R2) and NERC (grant number NE/G000883/1). The development of the humidity chamber has benefitted from key contributions from Dr. Mariana Ghosh and Dr. Sami Almabrok. The sample preparation of the oleic acid/sodium oleate mixtures has had important input from Jana Gessner and Cheng Yuan.

REFERENCES

- (1) Brandt, E. H. Acoustic Physics - Suspended by Sound. *Nature* **2001**, *413*, 474–475.
- (2) Marzo, A.; Seah, S. A.; Drinkwater, B. W.; Sahoo, D. R.; Long, B.; Subramanian, S. Holographic Acoustic Elements for Manipulation of Levitated Objects. *Nat. Commun.* **2015**, *6*, 8661.
- (3) Lierke, E. G.; Holitzner, L. Positioning of Drops, Particles and Bubbles in Ultrasonic Standing-Waves Levitators. A Final Round Up. *Acta Acust. Acust.* **2013**, *99*, 302–316.
- (4) Scheeline, A.; Behrens, R. L. Potential of Levitated Drops to Serve as Microreactors for Biophysical Measurements. *Biophys. Chem.* **2012**, *165*, 1–12.
- (5) Chainani, E. T.; Ngo, K. T.; Scheeline, A. Electrochemistry in an Acoustically Levitated Drop. *Anal. Chem.* **2013**, *85*, 2500–2506.
- (6) Chainani, E. T.; Choi, W.-H.; Ngo, K. T.; Scheeline, A. Mixing in Colliding, Ultrasonically Levitated Drops. *Anal. Chem.* **2014**, *86*, 2229–2237.
- (7) Bauerecker, S.; Neidhart, B. Atmospheric Physics - Cold Gas Traps for Ice Particle Formation. *Science* **1998**, *282*, 2211–2212.
- (8) Mason, N. J.; Drage, E. A.; Webb, S. M.; Dawes, A.; McPheat, R.; Hayes, G. The Spectroscopy and Chemical Dynamics of Micro-particles Explored Using an Ultrasonic Trap. *Faraday Discuss.* **2008**, *137*, 367–376.
- (9) Shen, C. L.; Xie, W. J.; Yan, Z. L.; Wei, B. Internal Flow of Acoustically Levitated Drops Undergoing Sectorial Oscillations. *Phys. Lett. A* **2010**, *374*, 4045–4048.
- (10) Tuckermann, R.; Bauerecker, S.; Cammenga, H. K. Generation and Characterization of Surface Layers on Acoustically Levitated Drops. *J. Colloid Interface Sci.* **2007**, *310*, 559–569.
- (11) Shen, C.; Xie, W.; Wei, B. Digital Image Processing of Sectorial Oscillations for Acoustically Levitated Drops and Surface Tension Measurements. *Sci. China: Phys., Mech. Astron.* **2010**, *53*, 2260–2265.
- (12) Delißen, F.; Leiterer, J.; Bienert, R.; Emmerling, F.; Thünemann, A. F. Agglomeration of Proteins in Acoustically Levitated Droplets. *Anal. Bioanal. Chem.* **2008**, *392*, 161–165.
- (13) Pieranski, P.; Sotta, P.; Rohe, D.; Imperor-Clerc, M. Devil's Staircase-type Faceting of a Cubic Lyotropic Liquid Crystal. *Phys. Rev. Lett.* **2000**, *84*, 2409–2412.
- (14) Richardson, S. J.; Staniec, P. A.; Newby, G. E.; Terrill, N. J.; Elliott, J. M.; Squires, A. M.; Gozdz, W. T. Predicting the Orientation of Lipid Cubic Phase Films. *Langmuir* **2014**, *30*, 13510–13515.
- (15) Rittman, M.; Amenitsch, H.; Rappolt, M.; Sartori, B.; O'Driscoll, B. M. D.; Squires, A. M. Control and Analysis of Oriented Thin Films of Lipid Inverse Bicontinuous Cubic Phases Using Grazing Incidence Small-Angle X-ray Scattering. *Langmuir* **2013**, *29*, 9874–9880.
- (16) Santesson, S.; Nilsson, S. Airborne Chemistry: Acoustic Levitation in Chemical Analysis. *Anal. Bioanal. Chem.* **2004**, *378*, 1704–1709.
- (17) Lopez-Pastor, M.; Dominguez-Vidal, A.; Ayora-Canada, M. J.; Laurell, T.; Valcarcel, M.; Lendl, B. Containerless Reaction Monitoring in Ionic Liquids by Means of Raman Microspectroscopy. *Lab Chip* **2007**, *7*, 126–132.
- (18) Radnik, J.; Bentrup, U.; Leiterer, J.; Brueckner, A.; Emmerling, F. Levitated Droplets as Model System for Spray Drying of Complex Oxides: A Simultaneous in Situ X-ray Diffraction/Raman Study. *Chem. Mater.* **2011**, *23*, 5425–5431.
- (19) Rehder, S.; Wu, J. X.; Laackmann, J.; Moritz, H.-U.; Rantanen, J.; Rades, T.; Leopold, C. S. A Case Study of Real-time Monitoring of Solid-state Phase Transformations in Acoustically Levitated Particles Using Near Infrared and Raman Spectroscopy. *Eur. J. Pharm. Sci.* **2013**, *48*, 97–103.
- (20) Brotton, S. J.; Kaiser, R. I. Novel High-temperature and Pressure-compatible Ultrasonic Levitator Apparatus Coupled to Raman and Fourier Transform Infrared Spectrometers. *Rev. Sci. Instrum.* **2013**, *84*, 055114.
- (21) Wolf, S. E.; Leiterer, J.; Kappl, M.; Emmerling, F.; Tremel, W. Early Homogenous Amorphous Precursor Stages of Calcium Carbonate and Subsequent Crystal Growth in Levitated Droplets. *J. Am. Chem. Soc.* **2008**, *130*, 12342–12347.
- (22) Troebs, L.; Nguyen Thi, Y.; Rump, D.; Emmerling, F. Crystallization Behavior of Carbamazepine. *Z. Phys. Chem.* **2014**, *228*, 493–501.
- (23) Benmore, C. J.; Weber, J. K. R.; Taylor, A. N.; Cherry, B. R.; Yarger, J. L.; Mou, Q.; Weber, W.; Neufeind, J.; Byrn, S. R. Structural Characterization and Aging of Glassy Pharmaceuticals Made Using Acoustic Levitation. *J. Pharm. Sci.* **2013**, *102*, 1290–1300.
- (24) Tiddy, G. J. T. Surfactant-water Liquid Crystal Phases. *Phys. Rep.* **1980**, *57*, 1–46.
- (25) Seddon, J.; Templer, R. Polymorphism of Lipid-water Systems. *Handb. Biol. Phys.* **1995**, *1*, 97–160.
- (26) Landau, E. M.; Rosenbusch, J. P. Lipidic Cubic Phases: A Novel Concept for the Crystallization of Membrane Proteins. *Proc. Natl. Acad. Sci. U. S. A.* **1996**, *93*, 14532–14535.
- (27) Milak, S.; Zimmer, A. Glycerol Monooleate Liquid Crystalline Phases Used in Drug Delivery Systems. *Int. J. Pharm.* **2015**, *478*, 569–587.
- (28) Attard, G. S.; Bartlett, P. N.; Coleman, N. R. B.; Elliott, J. M.; Owen, J. R.; Wang, J. H. Mesoporous Platinum Films from Lyotropic Liquid Crystalline Phases. *Science* **1997**, *278*, 838–840.
- (29) Akbar, S.; Elliott, J. M.; Rittman, M.; Squires, A. M. Facile Production of Ordered 3D Platinum Nanowire Networks with "Single Diamond" Bicontinuous Cubic Morphology. *Adv. Mater.* **2013**, *25*, 1160–1164.
- (30) Clerc, M.; Laggner, P.; Levelut, A. M.; Rapp, G. Rates Of Phase-Transformations Between Mesophases Formed By A Nonionic Surfactant In Water - A Time-Resolved X-Ray-Diffraction Study. *J. Phys. II* **1995**, *5*, 901–917.
- (31) Rappolt, M.; Di Gregorio, G. M.; Almgren, M.; Amenitsch, H.; Pabst, G.; Laggner, P.; Mariani, P. Non-equilibrium Formation of the Cubic Pn3m Phase in a Monoolein/water System. *Europhys. Lett.* **2006**, *75*, 267–273.
- (32) Brooks, N. J.; Ces, O.; Templer, R. H.; Seddon, J. M. Pressure Effects on Lipid Membrane Structure and Dynamics. *Chem. Phys. Lipids* **2011**, *164*, 89–98.
- (33) Oka, T. Transformation between Inverse Bicontinuous Cubic Phases of a Lipid from Diamond to Primitive. *Langmuir* **2015**, *31*, 3180–3185.
- (34) Pereira-Lachataignerais, J.; Pons, R.; Amenitsch, H.; Rappolt, M.; Sartori, B.; Lopez, O. Effect of Sodium Dodecyl Sulfate at Different Hydration Conditions on Dioleoyl Phosphatidylcholine Bilayers Studied by Grazing Incidence X-ray Diffraction. *Langmuir* **2006**, *22*, 5256–5260.
- (35) Richardson, S. J.; Staniec, P. A.; Newby, G. E.; Rawle, J. L.; Slaughter, A. R.; Terrill, N. J.; Elliott, J. M.; Squires, A. M. Glycerol Prevents Dehydration in Lipid Cubic Phases. *Chem. Commun.* **2015**, *51*, 11386–11389.
- (36) Asghar, K. Ph.D. Thesis, University of Reading, 2012.
- (37) Latypova, L.; Gozdz, W. T.; Pieranski, P. Facets of Lyotropic Liquid Crystals. *Langmuir* **2014**, *30*, 488–495.
- (38) Gras, S. L.; Squires, A. M. Dried and Hydrated X-ray Scattering Analysis of Amyloid Fibrils. *Methods Mol. Biol.* **2011**, *752*, 147–163.